GEOPHYSICAL RESEARCH LETTERS, VOL. 23, NO. 24, PAGES 3527-3530, DECEMBER 1, 1996

Hot mantle transition zone beneath Iceland and the adjacent Mid-Atlantic Ridge inferred from P-to-S conversions at the 410- and 660-km discontinuities

Yang Shen[1], Sean C. Solomon[2], Ingi Th. Bjarnason[2,3], and G. M. Purdy[1,4]

Abstract. *P*-to-*S* conversions from the two primary discontinuities near 410 and 660 km depth (*P410s* and *P660s* phases) are evident in particle motions and receiver functions of teleseismic body waves recorded by broadband seismic stations in Iceland. The average arrival times of *P410s* and *P660s* are later by 7.0 ± 0.5 s (standard error) and 4.7 ± 0.2 s, respectively, than predicted by the *iasp91* Earth model. Differential *P660s* -*P410s* travel times indicate that the upper mantle transition zone between the 410- and 660-km discontinuities is 23 ± 9 km thinner than in the *iasp91* model. From estimates for the Clapeyron slopes of the phase transitions associated with these discontinuities, this lesser transition zone thickness is consistent with temperatures 180 ± 70 K hotter than normal. We interpret this result as evidence for upwelling mantle flow at 400-700 km depth beneath Iceland and the adjacent Mid-Atlantic Ridge.

Introduction

The locations of the two primary upper mantle seismic discontinuities at about 410 km and 660 km depth provide important information on mantle temperature structure and its variations, and thus on the influence of mantle convection on the temperature field. The 410-km discontinuity is identified with the transformation of (Mg, Fe)$_2$SiO$_4$ from the olivine (α-phase) to the modified spinel (β-phase) structure, and the 660-km discontinuity with the transformation of (Mg, Fe)$_2$SiO$_4$ in the spinel (γ-phase) structure to (Mg, Fe)SiO$_3$ in the perovskite structure plus (Mg, Fe)O [e.g., *Bina and Helffrich,* 1994]. The depths to the 410-km and 660-km discontinuities respectively increase and decrease with increasing temperature. While significant progress has been made in mapping these discontinuities both globally and in higher-resolution studies of several subduction zone regions from observations of reflected or converted body waves [e.g., *Shearer*, 1991; *Vidale and Benz*, 1992; *Wicks and Richards*, 1993], comparatively little is known about the depths of these discontinuities beneath hotspots and mid-ocean ridges, the most likely sites of upwelling within the mantle transition zone. *Nakanishi* [1988] reported observations of *P'P'* precursors inferred to be underside reflections from the two discontinuities about 200-400 km from the axis of the Mid-Atlantic Ridge, but the depths of the discontinuities were poorly constrained. In studies of these discontinuities in oceanic areas relying on observations of precursors to long-period *SS* waves [*Shearer*, 1991; *Lee and Grand*, 1996], sampling of mid-ocean ridges and hotspots is generally sparse, and the horizontal resolution (at best about 1000 km) is inadequate to resolve lateral variations in discontinuity depths beneath such regions, which likely occur on scales of a few hundred kilometers or less.

In this paper we report observations of *P410s* and *P660s* phases, shear waves converted from teleseismic *P* waves at 410 and 660 km depth, respectively, from a broadband seismic network in Iceland. The network consists of five portable Streckeisen STS-2 seismometers installed during the first phase of the ICEMELT experiment [*Bjarnason et al.*, 1996] and the permanent Global Seismographic Network station BORG (Figure 1). Utilizing particle motion and receiver function analyses, we examined teleseismic body wave records from these stations for the period August 1993 through December 1994 for evidence of upper mantle *P*-to-*S* conversions. The arrival times of documented *P660s* and *P410s* phases provide new constraints on the mantle thermal structure and flow field beneath this prominent ridge-centered hotspot.

Particle Motions

The particle motion of a converted *S* wave is distinctly different from that of the *P* wave and thus provides a key to phase identification [*Sacks and Snoke*, 1977]. Teleseismic *P* waves are steeply incident and dominate the vertical component of ground motion, whereas the *Pds* phase (where *d* is the conversion depth) appears principally on the radial component. Observed particle motions (Figure 2) are compared with that predicted for the *iasp91* model [*Kennett and Engdahl*, 1991], modified to include a 25-km-thick crust having the *P* wave velocity structure obtained for southern Iceland by *Bjarnason et al.* [1993] and a V_P/V_S ratio of 1.75. The synthetic seismogram has been calculated using the reflectivity method [*Müller*, 1985]. The Harvard centroid moment tensor solution was adopted as the focal mechanism, and the reflectivity response was convolved with the instrument response and a moment function as defined by *Brüstle and Müller* [1983] with a source duration of 10 s.

The near horizontal motion of the *P660s* phase, which arrives about 67 s after *P*, is clearly discernible in the synthetic particle motion. A similar phase, with identical polarity but arriving 4-6 s later than in the synthetic, is also evident in the data (Figure 2). This arrival, which we identify as *P660s*, is absent in the transverse components of records from this event. At the low frequencies of these seismograms, filtered to clarify the *P660s* phase in the observed records, the *P*-to-*S* conversion from the 410-km discontinuity (*P410s*) is not evident, even in the synthetic.

[1] Department of Geology and Geophysics, Woods Hole Oceanographic Institution, Woods Hole, Mass.
[2] Department of Terrestrial Magnetism, Carnegie Institution of Washington, Washington, D. C.
[3] Science Institute, University of Iceland, Reykjavík
[4] Now at Division of Ocean Sciences, National Science Foundation, Arlington, Va.

Paper number 96GL03371.
0094-8534/96/96GL-03371$05.00

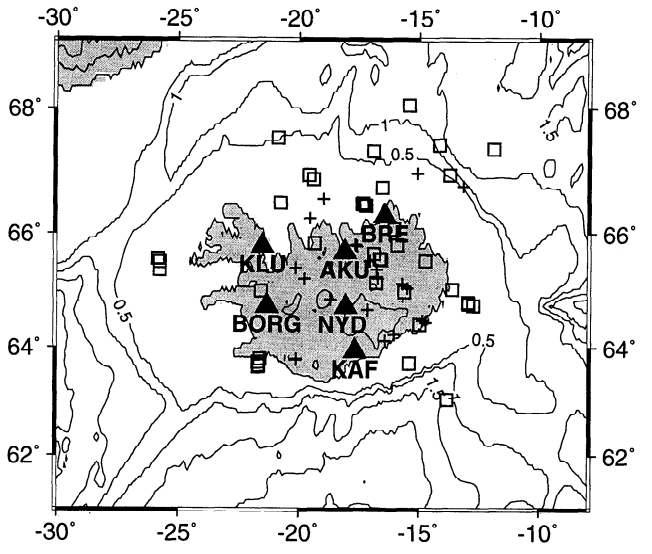

Figure 1. Broadband seismic stations used (solid triangles) and conversion points of identified *P660s* (open squares) and *P410s* (crosses) arrivals. Shaded areas are above sea level. Bathymetric contours are in kilometers. See *Bjarnason et al.* [1996] for more information on the five ICEMELT stations.

Receiver Functions

On the basis of the identification of converted phases from particle motions, we employ receiver function analysis [e.g., *Langston*, 1979; *Ammon*, 1991] to estimate arrival times. Example receiver functions (obtained from the seismograms for which particle motions are plotted in Figure 2) are shown in Figure 3. *P660s* is a pronounced phase in the individual receiver functions and in a straight stack of the four receiver functions. The arrival times of *P660s* in the receiver functions are consistent with the times of arrival of near-horizontal particle motion in Figure 2. *P410s* can be identified in the receiver function for one station but not in the others.

The large amplitudes of the identified *P660s* and *P410s* phases (5-15% and 4-12%, respectively, of the amplitude of the vertical component *P* wave) are most likely the consequence of focusing and defocusing of the converted phases by relief on the discontinuities [e.g., *van der Lee et al.*, 1994]. Supporting this inference are the frequently significant variations in the amplitude of a given converted phase seen in receiver functions for the same event (e.g., *P660s* in Figure 3) and instances where a converted phase is evident in one receiver function yet not in others from the same earthquake (e.g., *P410s* in Figure 3).

We utilized a total of 47 receiver functions from records of earthquakes at epicentral distances between 50° and 110°

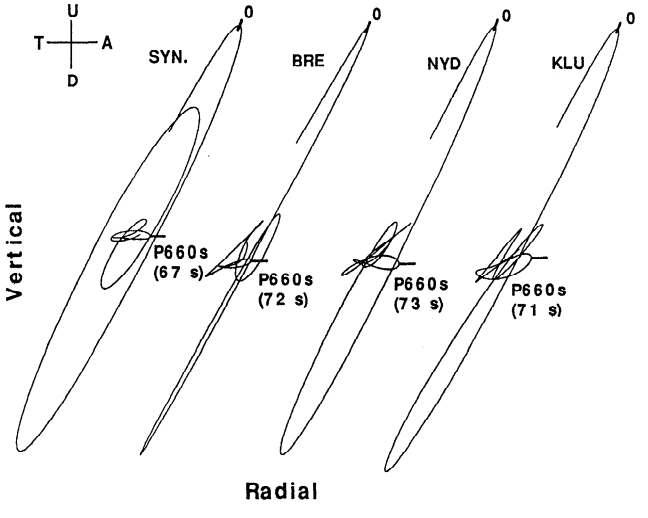

Figure 2. Synthetic (SYN) and observed (BRE, NYD, and KLU) particle motions of the *P*-wave codas from the Kuril Islands earthquake of 9 October 1994 (m_b 6.5, focal depth 22 km, epicentral distances 69.5-71.9°). Vertical motion is marked U and D (up and down); radial horizontal motion T and A (toward and away from the source). Both the synthetic (see text) and observed seismograms have been low-pass filtered at 0.05 Hz. The times of maximum amplitude of the *P* waves are marked by a zero; differential times between maximum amplitudes of *P* and *P660s* phases are given in parentheses.

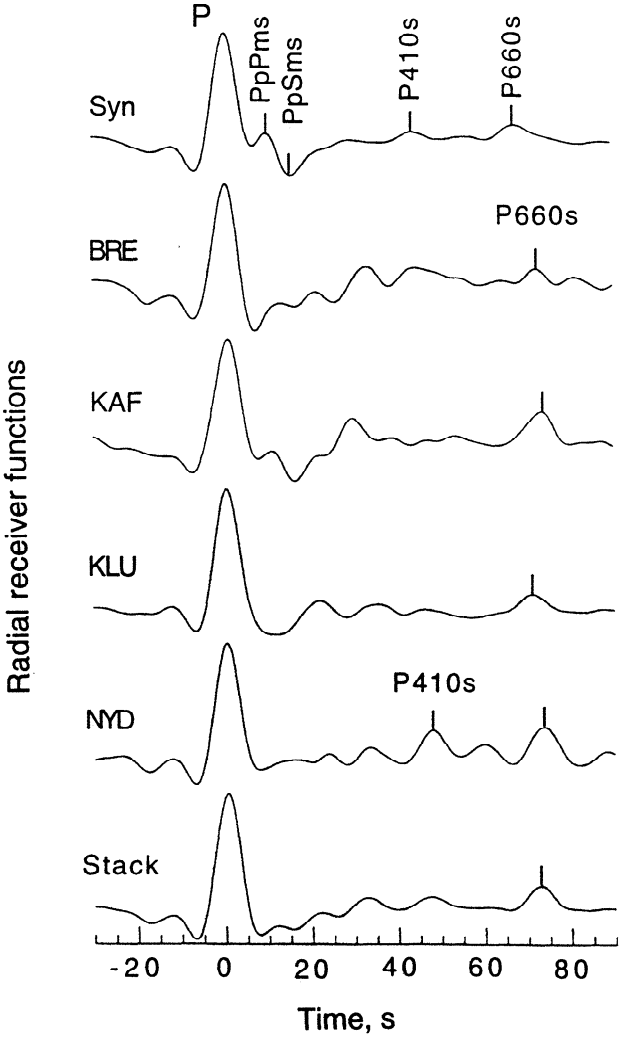

Figure 3. Synthetic and observed radial receiver functions for the Kuril Islands earthquake of 9 October 1994. Converted phases are indicated by tick marks. The synthetic receiver function is calculated for the modified *iasp91* model as in Figure 2. In the deconvolution for receiver functions [*Ammon*, 1991], the minimum allowed spectral amplitude of the vertical component (0.01) and the Gaussian width factor (0.3, equivalent to low-pass filtering at 0.13 Hz) have been selected on the basis of presignal noise and separation of converted phases. Phase nomenclature is after *Langston* [1979].

having clear *P* or *PP* arrivals. Time windows were chosen so that the *P* coda does not contain *PP*, or the *PP* coda *PPP*. Care was taken to avoid seismograms with other visible arrivals having ray parameters significantly different from those of *P* and *PP*. In the following discussion, for simplicity, we make no further distinction between *P* and *PP* or between *Pds* and *PPds*. Phases in these receiver functions that arrive between 35 and 85 s after the reference phase and have amplitudes greater than presignal noise generally fall into one of two distinct time intervals: 45-55 s and 66-76 s. We identify such arrivals as *P410s* and *P660s*, respectively, if their signal-to-noise ratios are greater than 1.5. On the basis of the dominant periods and the signal-to-noise ratios of the converted phases, we estimate that arrival times of *P660s* phases can be picked to within 1-1.5 s, and those of *P410s* to within 1.5-2 s.

Converted Phase Arrival Times

The arrival times of 22 and 40 identified *P410s* and *P660s* phases, respectively, are shown in Figure 4a as functions of ray parameter (a greater ray parameter corresponds to a longer converted wave path above the discontinuity). Two aspects of the observations are noteworthy. First, the arrival times are significantly later than those predicted for the *iasp91* model, as modified above. Second, the times show significant scatter, up to 6 s, for a given ray parameter (but different *P*-to-*S* conversion locations). Measurements of arrival times of direct *S* and *SKS* waves across the ICEMELT network [*Bjarnason et al.*, 1996] suggest that lateral variations in upper mantle structure may contribute as much as 3-4 s to the scatter in the arrival times of the converted phases. Relief on the discontinuities may also add to the variations in arrival times.

Using the moveout of the *iasp91* model, we correct the arrival times in Figure 4a to a single reference ray parameter of 0.0573 s/km (corresponding to an epicentral distance of 67° for a focal depth of 33 km). The correction is only weakly dependent on upper mantle velocity; a 10% lower velocity in the upper 410 km would result in only 0.2 s less moveout for the *P660s* phase between ray parameters of 0.0573 and 0.075 s/km, and 0.15 s less moveout for *P410s*. The average delay for the *P660s* phase is 4.7 s, with a standard deviation of 1.4 s and a standard error of the mean (estimated by bootstrap resampling of the 40 *P660s* arrival times) of 0.2 s. The average delay for the *P410s* phase with respect to the *iasp91* model is 7.0 s, with a standard deviation of 2.3 s and a standard error of the mean of 0.5 s. The standard errors of the mean are likely to underestimate the true uncertainties, because our data set may be biased to situations favoring high-amplitude arrivals and there is only limited and uneven spatial coverage of conversion points (Figure 1).

From discontinuity-converted phases observed at a number of primarily continental sites, *Stammler et al.* [1992] found that the arrival times of *P660s* and *P410s* are positively correlated and covary with a slope near unity. *Stammler et al.* [1992] inferred that most of the variation in both the *P660s* and *P410s* times (Figure 4b) is contributed by mantle structure above 410 km depth (where the two phases have similar paths). The average arrival times for *P660s* and *P410s* for Iceland (Figure 4b) greatly extend the spread of known arrival times for these phases. These average times, however, do not lie on the line of unit slope through the point for *iasp91* and the data of *Stammler et al.* [1992].

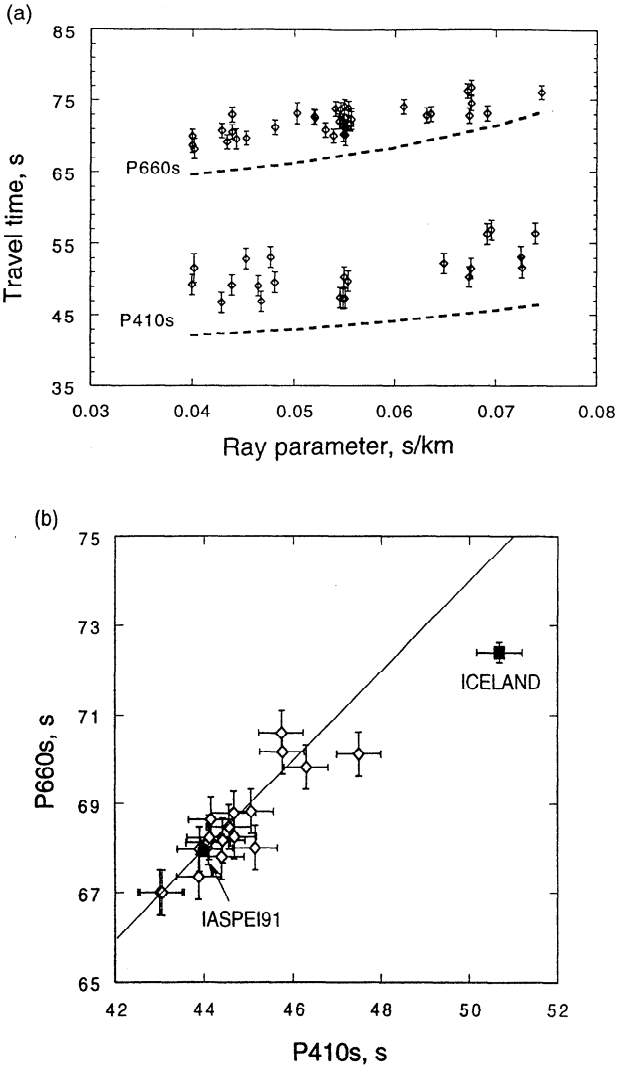

Figure 4. (a) Observed (diamonds) and predicted (dashes) arrival times of *P660s* and *P410s* versus ray parameter. The predicted times have been calculated by ray tracing through the modified *iasp91* model. Error bars denote estimated picking errors. (b) A comparison of average *P660s* and *P410s* arrival times for Iceland (solid square) with those from other geological regions (diamonds) reported by *Stammler et al.* [1992]. The error bars for Iceland data are standard errors of the means; those for the other regions are 1-σ errors in the arrival times of the converted phases obtained from receiver function stacks. The line shown has a slope of 1 and satisfies the predicted times for the (unmodified) *iasp91* model (dot).

Thinner and Hotter Mantle Transition Zone

Because lateral variations in mantle temperature are expected to produce anticorrelated variations in the depths to the 410- and 660-km discontinuities [*Bina and Helffrich*, 1994], the most likely interpretation of the greater delay in *P410s* than in *P660s* is that the depth interval between the two discontinuities is less than the global mean value. To test this suggestion, as well as the alternative possibility that the difference arises from different sets of wave paths for our observations of the two phases, we examined differential times between *P660s* and *P410s* on individual receiver functions on which both phases are seen (e.g., NYD in Figure 3). Since the

paths for such paired converted phases above 410 km depth are nearly identical, the differential times reflect the thickness and velocity of the upper mantle transition zone. Referenced to a ray parameter of 0.0573 s/km, the average differential time of 14 pairs is 22.1 s, with a standard deviation of 2.8 s and a standard error of the mean of 0.9 s. This value is consistent with the difference between the average arrival times (21.7 ± 0.7 s; see Figure 4b). The average differential time is 2.3 ± 0.9 s smaller than the value predicted for the *iasp91* model.

The implied transition zone thickness is less than in *iasp91* by 23 ± 9 km (standard error), and points to a deeper than normal 410-km discontinuity, a shallower than average 660-km discontinuity, or both. For comparison, the transition zone thickness we derive beneath Iceland is less by 16 ± 9 km than that obtained by *Shearer* [1996] from long-period *SS* precursors in oceanic regions. If the *S* wave velocity between 410 and 660 km depth beneath Iceland is lower than in the reference models, an even thinner transition zone is implied (a 2% lower velocity in the mantle transition zone would increase the differential travel time by 0.4 s). Recent estimates of the Clapeyron slopes for the phase transitions associated with the 410- and 660-km discontinuities [*Bina and Helffrich*, 1994] permit us to convert the difference in transition zone thickness to an estimate of the excess temperature of the transition zone beneath Iceland. For Clapeyron slopes of 2.9 MPa/K for the 410-km discontinuity and -2.1 MPa/K for the 660-km discontinuity [*Bina and Helffrich*, 1994], the lesser mantle transition zone thickness beneath the Iceland region than in the *iasp91* model is consistent with an excess temperature of 180 ± 70 K. Our results thus support the inference that high temperatures associated with mantle upwelling beneath Iceland extend to depths as great as 400-700 km.

The converted phases sample a broad area (Figure 1), so the transition zone thickness obtained here represents an average over a region that may be larger than the Iceland hotspot or the Mid-Atlantic Ridge axial zone. *P*- and *S*-wave tomography of the upper mantle beneath Iceland, for instance, indicates that the Iceland plume at depths of 100-400 km has a diameter of no more than about 300 km [*Wolfe et al.*, 1996]. On the basis of numerical models for the penetration of a plume through a mantle phase boundary, however, the zone of anomalous temperatures near the transition zone may be much broader than the diameter of the plume well above or below the transition zone [*Davies*, 1995].

The excess temperature derived above from the average transition zone thickness beneath the Iceland region is in general agreement with other estimates of the thermal anomaly of the plume at shallower depths. Analyses of basalt chemistry and crustal thickness [e.g., *White et al.*, 1995] suggest that the temperature anomaly beneath Iceland is about 150-200 K at the depth of melt generation (shallower than 200 km). *P*- and *S*-wave velocities at 100-400 km depth within the core of the Iceland mantle plume [*Wolfe et al.*, 1996] are consistent with excess temperatures of 200-300 K, although these figures depend strongly on the uncertain conversion between velocities and temperature.

Acknowledgments. We are grateful to R. Kuehnel for assistance with field operations, C. J. Wolfe for help with data processing, and S. van der Lee for providing software. We also thank J. A. Collins, R. S. Detrick, D. W. Forsyth, G. M. Kent, G. Nolet, I. S. Sacks, P. G. Silver, P. D. Slack, J. C. VanDecar, and C. J. Wolfe for helpful discussions, and A. F. Sheehan, J. E. Vidale, and an anonymous reviewer for constructive reviews. This work was supported by a WHOI Postdoctoral Fellowship and the National Science Foundation under grants EAR-9316137 and OCE-9403697. WHOI contribution 9358.

References

Ammon, C. J., The isolation of receiver effects from teleseismic *P* waveforms, *Bull. Seism. Soc. Am., 81*, 2504-2510, 1991.

Bina, C. R., and G. Helffrich, Phase transition Clapeyron slopes and transition zone seismic discontinuity topography, *J. Geophys. Res., 99*, 15,853-15,860, 1994.

Bjarnason, I. Th., W. Menke, Ó. G. Flóvenz, and D. Caress, Tomographic image of the Mid-Atlantic plate boundary in southwestern Iceland, *J. Geophys. Res., 98*, 6607-6622, 1993.

Bjarnason, I. Th., C. J. Wolfe, S. C. Solomon, and G. Gudmundson, Initial results from the ICEMELT experiment: Body-wave delay times and shear-wave splitting across Iceland, *Geophys. Res. Lett., 23*, 459-462, 1996; Correction, *Geophys. Res. Lett., 23*, 903, 1996.

Brüstle, W., and G. Müller, Moment and duration of shallow earthquakes from Love-wave modelling for regional distances, *Phys. Earth Planet. Inter., 32*, 312-324, 1983.

Davies, G. F., Penetration of plates and plumes through the mantle transition zone, *Earth Planet. Sci. Lett., 133*, 507-516, 1995.

Kennett, B. L. N., and E. R. Engdahl, Travel times for global earthquake location and phase identification, *Geophys. J. Int., 105*, 429-466, 1991.

Langston, C. A., Structure under Mount Rainier, Washington, inferred from teleseismic body waves, *J. Geophys. Res., 84*, 4749-4762, 1979.

Lee, D.-K., and S. P. Grand, Depths of the upper mantle discontinuities beneath the East Pacific Rise, *Geophys. Res. Lett.*, in press, 1996.

Müller, G., The reflectivity method: A tutorial, *J. Geophys., 58*, 153-174, 1985.

Nakanishi, I., Reflections of *P'P'* from upper mantle discontinuities beneath the Mid-Atlantic Ridge, *Geophys. J., 93*, 335-346, 1988.

Sacks, I. S., and J. A. Snoke, The use of converted phases to infer the depth of the lithosphere-asthenosphere boundary beneath South America, *J. Geophys. Res., 82*, 2011-2017, 1977.

Shearer, P. M., Constraints on upper mantle discontinuities from observations of long-period reflected and converted phases, *J. Geophys. Res., 96*, 18,147-18,182, 1991.

Shearer, P. M., Transition zone velocity gradients and the 520-km discontinuity, *J. Geophys. Res., 101*, 3053-3066, 1996.

Stammler, K., R. Kind, N. Petersen, G. Kosarev, L. Vinnik, and L. Qiyuan, The upper mantle discontinuities: Correlated or anticorrelated?, *Geophys. Res. Lett., 19*, 1563-1566, 1992.

Vidale, J. E., and H. M. Benz, Upper-mantle seismic discontinuities and the thermal structure of subduction zones, *Nature, 356*, 678-683, 1992.

van der Lee, S., H. Paulssen, and G. Nolet, Variability of *P660s* phases as a consequence of topography of the 660 km discontinuity, *Phys. Earth Planet. Inter., 86*, 147-164, 1994.

White, R. S., J. W. Bown, and J. R. Smallwood, The temperature of the Iceland plume and origin of outward-propagating V-shaped ridges, *J. Geol. Soc. Lond., 152*, 1039-1045, 1995.

Wicks, C. W., Jr., and M. A. Richards, A detailed map of the 660-kilometer discontinuity beneath the Izu-Bonin subduction zone, *Science, 261*, 1424-1427, 1993.

Wolfe, C. J., I. Th. Bjarnason, J. C. VanDecar, and S. C. Solomon, Seismic structure of the Iceland mantle plume, *Nature*, in press, 1996.

I. Th. Bjarnason, Science Institute, Dunhaga 5, University of Iceland, 107 Reykjavík, Iceland.

G. M. Purdy, Division of Ocean Sciences, National Science Foundation, 4201 Wilson Boulevard, Arlington, VA 22230.

S. C. Solomon, Department of Terrestrial Magnetism, Carnegie Institution of Washington, 5241 Broad Branch Road, N. W., Washington, DC 20015.

Y. Shen, Department of Geology and Geophysics, Woods Hole Oceanographic Institution, Woods Hole, MA 02543.

(Received April 4, 1996; revised September 5, 1996;
accepted September 25, 1996.)